INTERNATIONAL JOURNAL FOR NUMERICAL METHODS IN FLUIDS, VOL. 25, 249–263 (1997)

AN EVALUATION OF THE BOUNCE-BACK BOUNDARY CONDITION FOR LATTICE BOLTZMANN SIMULATIONS

MARTHA A. GALLIVAN, DAVID R. NOBLE,* JOHN G. GEORGIADIS AND RICHARD O. BUCKIUS

Department of Mechanical and Industrial Engineering, University of Illinois at Urbana-Champaign, Urbana, IL 61801, U.S.A.

SUMMARY

The bounce-back boundary condition for lattice Boltzmann simulations is evaluated for flow about an infinite periodic array of cylinders. The solution is compared with results from a more accurate boundary condition formulation for the lattice Boltemann method and with finite difference solutions. The bounce-back boundary condition is used to simulate boundaries of cylinders with both circular and octagonal cross-sections. The convergences of the velocity and total drag associated with this method are slightly sublinear with grid spacing. Error is also a function of relaxation time, increasing exponentially for large relaxation times. However, the accuracy does not exhibit a trend with Reynolds number between 0·1 and 100. The square lattice Boltzmann grid conforms to the octagonal cylinder but only approximates the circular cylinder, and the resulting error associated with the octagonal cylinder is half the error of the circular cylinder. The bounce-back boundary condition is shown to yield accurate lattice Boltzmann simulations with reduced computational requirements for computational grids of 170×170 or finer, a relaxation time less than 1·5 and any Reynolds number from 0·1 to 100. For this range of parameters the root mean square error in velocity and the relative error in drag coefficient are less than 1 per cent for the octagonal cylinder and 2 per cent for the circular cylinder.

Int. J. Numer. Meth. Fluids, **25**: 249–263 (1997).

No. of Figures: 11. No. of Tables: 0. No. of References: 20.

KEY WORDS: lattice Boltzmann; boundary conditions; bounce-back; accuracy

1. INTRODUCTION

The increased use of the lattice Boltzmann method (LBM)[1–5] for the computation of fluid flow has generated the need for more rigorous documentation of the errors associated with the LBM. An important and significant source of error stems from the conditions and constraints imposed upon the boundary of an obstacle in the flow. The most commonly used LBM boundary condition is known as the bounce-back method,[6–9] which is the topic of this study. Although this method does not provide high-accuracy boundary conditions for the fluid particle distribution, it does provide reasonably accurate flow solutions for a range of discretization parameters. Recently a number of more accurate

* Correspondence to: D. R. Noble, Sondia National Laboratories. P.O. Box 5800, Albuquerque, NM 87185-0826, USA

Contract grant sponsor: National Science Foundation Graduate Fellowship
Contract grant sponsor: NCSA; Contract grant number: CBT-930030N
Contract grant sponsor: NSF; Contract grant number: CTS 95-21509
Contract grant sponsor: Richard W. Kritzer Foundation

CCC 0271–2091/97/030249–15 $17.50

Received 14 June 1996
Revised 3 October 1996

but more computationally intensive lattice Boltzmann boundary conditions have been proposed.[10–12] The consistent hydrodynamic boundary condition proposed by Noble *et al.*[13–15] produces less error and demonstrates a formally second-order rate of error convergence with grid resolution; for these reasons it is used as an accurate solution in this study. However, this boundary condition demands more computational resources and cannot be easily extended to arbitrary surface geometries. As a result, the bounce-back boundary condition may be a preferable method for modelling no-slip boundaries if the error associated with that particular flow is acceptable.

In this study the flow through a two-dimensional periodic array of infinite parallel cylinders is considered. The two types of cylinders investigated in this study are octagonal and circular in cross-section. This work documents the accuracy associated with the bounce-back boundary condition through the calculation of errors in local velocity, local viscous drag and total drag. Accuracy is computed as a function of grid resolution, relaxation time and Reynolds number.

2. THEORY

2.1. Lattice Boltzmann method

The lattice Boltzmann method is a kinetic-theory-based technique for modelling fluid flow and is formulated in terms of the probability of the existence of a fluid particle in the vicinity of a given location and time that is moving in one of a number of discrete directions. In this study a two-dimensional square grid lattice is utilized, so that each node is linked to eight neighbours, those immediately horizontal, vertical and diagonal. The discrete directions are described by the eight velocity vectors

$$\mathbf{e}_i = \frac{\Delta x}{\Delta t}\left[\cos\left(\frac{2\pi(i-1)}{8}\right), \sin\left(\frac{2\pi(i-1)}{8}\right)\right], \quad i = 1, 2, \ldots, 8, \tag{1}$$

where Δx is the grid spacing and Δt is the time step. The particle distribution f_i is a function of location and time, denoted $\mathbf{x}$ and t, as well as the discrete velocities described by the vectors $\mathbf{e}_i$. A rest particle distribution f_0 is also included. The particle distribution is described by the discrete velocity Boltzmann equation as

$$\frac{\partial f_i}{\partial t} + \mathbf{e}_i \cdot \nabla f_i = \Omega_i(f(\mathbf{x}, t)) + F_i, \tag{2}$$

where Ω_i is the collision operator and F_i is a term used to impose a uniform external body force.[12] For the flows discussed in this study, the body force is applied in the x-direction, which is defined as the streamwise direction. The particle collisions are described by the linearized, single-time relaxation model of Bhatnagar *et al.*[16] applied to the LBM model:[4]

$$\Omega_i(f) = -\frac{1}{\tau}(f_i - f_i^{\mathrm{eq}}), \tag{3}$$

where τ is the relaxation time which characterizes the rate at which the system relaxes towards the equilibrium distribution f_i^{eq}.

Using a Lagrangian discretization of (2) and substituting the collision model and body force provides the final form of the lattice Boltzmann evolution equation:

$$f_i(\mathbf{x} + \mathbf{e}_i\Delta t, t + \Delta t) = f_i(\mathbf{x}, t) + \frac{1}{\tau^*}[f_i^{\mathrm{eq}}(\mathbf{x}, t) - f_i(\mathbf{x}, t)] + F_i', \tag{4}$$

where $\tau^* = \tau/\Delta t$ is the dimensionless relaxation time and the body force term[12] $F_i' = F_i/\Delta t$ is given by

$$F_1' = F_2' = F_8' = \frac{|\mathbf{F}|}{6}\frac{(\Delta t)^2}{\Delta x}, \qquad F_4' = F_5' = F_6' = -\frac{|\mathbf{F}|}{6}\frac{(\Delta t)^2}{\Delta x}, \qquad F_0' = F_3' = F_7' = 0. \tag{5}$$

The macroscopic properties of the flow, including density ρ, velocity $\mathbf{u}$ and internal energy ε, are obtained by taking the moments of the particle distribution:

$$\sum_i f_i = \rho, \tag{6}$$

$$\sum_i f_i \mathbf{e}_i = \rho \mathbf{u}, \tag{7}$$

$$\tfrac{1}{2}\sum_i f_i(\mathbf{u} - \mathbf{e}_i)\cdot(\mathbf{u} - \mathbf{e}_i) = \rho\varepsilon \tag{8}$$

The incompressible Navier–Stokes fluid equations are recovered when the Boltzmann transport equation is truncated to its long-wavelength, low-frequency, low-Mach-number limit.[3] The equilibrium distribution used here is

$$f_0^{\mathrm{eq}} = \rho\left(\frac{2}{7} - \frac{2}{3c^2}(\mathbf{u}\cdot\mathbf{u})\right), \tag{9}$$

$$f_i^{\mathrm{eq}} = \rho\left(\frac{1}{7} + \frac{1}{3c^2}(\mathbf{e}_i\cdot\mathbf{u}) + \frac{1}{2c^4}(\mathbf{e}_i\cdot\mathbf{u})^2 - \frac{1}{6c^2}(\mathbf{u}\cdot\mathbf{u})\right), \tag{10}$$

$$f_i^{\mathrm{eq}} = \rho\left(\frac{1}{28} + \frac{1}{12c^2}(\mathbf{e}_i\cdot\mathbf{u}) + \frac{1}{8c^4}(\mathbf{e}_i\cdot\mathbf{u})^2 - \frac{1}{24c^2}(\mathbf{u}\cdot\mathbf{u})\right), \tag{11}$$

where $c = \Delta x/\Delta t$. The fluid properties of viscosity v and speed of sound c_s are given by

$$v = \frac{2\tau^* - 1}{6}\frac{(\Delta x)^2}{\Delta t}, \tag{12}$$

$$c_s = \sqrt{\left(\frac{3}{7}\right)}\frac{\Delta x}{\Delta t} \tag{13}$$

2.2. *Boundary conditions*

The implementation of the no-slip boundary condition studied in this paper is referred to as the 'bounce-back' method. To generate the solid boundary of an obstacle, links between neighbouring nodes are selected to best confirm to the shape of the obstacle. The nodes just outside the boundary no longer communicate with their neighbours inside the obstacle. Instead, a particle striking this boundary bounces back in the direction from which it arrived. Figure 1 shows one quadrant of the coarsest computational grid used for the octagonal and circular cylinders. The nodes at which the boundary condition is applied are shown. The bounce-back boundary condition is known to model, to first order, a boundary which lies halfway between these boundary nodes and the neighbouring fluid nodes.[7] Based on this interpretation, the approximate shapes of the obstacles being modelled are also indicated. The computational domain is devised such that the width of the cylinders is equal to the distance between the cylinders. It is apparent that the boundary condition cannot directly model a general curvilinear surface but instead uses a stair-step approximation of the surface. It is expected, however, that the accuracy is improved when modelling a surface which follows the grid lines, including the diagonal grid lines included in the two-dimensional square grid.

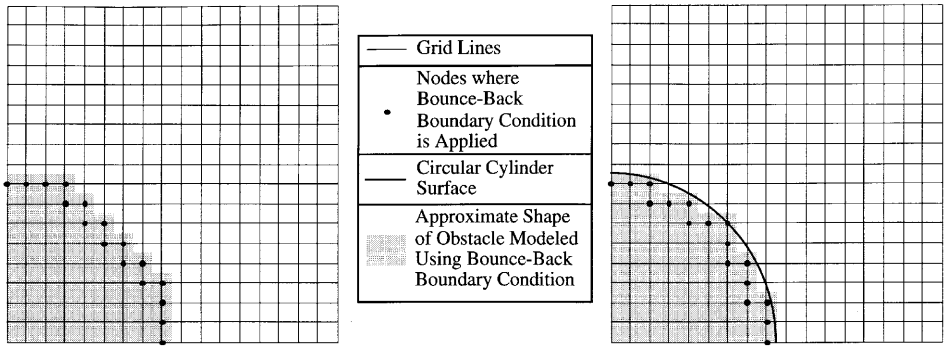

Figure 1. Implementation of bounce-back boundary condition for octagonal and circular cylinders. The approximate shape of the obstacle being modelled is shown based on the interpretation that the bounce-back boundary condition provides a surface lying halfway between the nodes where the boundary condition is applied and neighbouring fluid nodes. Note that the diagonal grid lines are not shown but also exist for the two-dimensional square grid

The bounce-back boundary condition is implemented in the lattice Boltzmann scheme after the particle distribution is updated according to (4). The application of (4) near the boundary causes some of the components of the distribution just inside the boundary to be non-zero. After the particle distribution is computed, the boundary condition reverses the direction of each component of the particle distribution just inside the boundary. These components then leave the boundary during the following time step. For example, a particle travelling in the direction $\mathbf{e}_1$ is bounded back in the opposite direction $\mathbf{e}_5$, so that the particle distributions f_1 and f_5 are interchanged. The LBM directional pairs f_2 and f_6, f_3 and f_7, and f_4 and f_8 are similarly reversed during the implementation of the bounce-back boundary condition.

The bounce-back boundary condition was originally developed to complement the lattice gas method for modelling viscous flow. In the lattice gas model the particle distribution function is a Boolean expression instead of a floating point probability distribution, representing only the presence or absence of a particle. As the lattice Boltzmann method evolved from the lattice gas model, the bounce-back boundary condition remained the default representation of an obstacle and is commonly used today in lattice Boltzmann computations. However, it is known[7–9] that the bounce-back boundary condition does not accurately describe the particle distribution in the fluid near a solid wall and is a heuristic method whose appeal lies in its simplicity and computational efficiency.

A more fundamentally based lattice Boltzmann boundary condition [13–15] provides constraints for the components of the particle distribution which are unknown at the wall. A full set of constraints is developed for the two-dimensional square grid in terms of the velocity boundary conditions to be imposed by assuming constant internal energy. This consistent hydrodynamic boundary condition (HBC) exhibits second-order convergence with grid size.[13,14] Lattice Boltzmann computations utilizing this boundary condition are used as a standard for comparison for the octagonal cylinders in this study. The consistent hydrodynamic boundary condition is more computationally demanding than the bounce-back method, but this is offset by its increased accuracy. In flow around an octagonal cylinder the calculations associated with the HBC consume approximately 25 per cent of the total processing time. By comparison the bounce-back boundary condition consumes less than 1 per cent of the computer time.

3. RESULTS AND DISCUSSION

The problem under consideration is the flow of fluid about a periodic array of cylinders which are octagonal and circular in cross-section. The flow field is computed by simulating the flow about a single cylinder while imposing periodicity at each of the domain boundaries. Lattice Boltzmann solutions for a range of grid size, Reynolds number and relaxation time are compared at each node in the field with the most accurate solutions obtained with improved schemes and the differences in velocity are computed. The maximum error in velocity is identified for each simulation and the global error is represented with the root mean square norm of the velocity error. The HBC lattice Boltzmann computations were used in this study as the accurate solutions for the octagonal cylinders. Based on the documented accuracy of the method for flow about a periodic array of cylinders[15] and the rate of convergence of the method, a 1020×1020 simulation using the HBC is expected to be accurate to within 0·05 per cent. However, the HBC cannot readily be adapted to arbitrary boundary geometries, because there are insufficient constraints for prescribing the components of the particle distribution which originate from outside the fluid domain. Therefore the bounce-back lattice Boltzmann solutions for the circular cylinders are compared with results from an alternating direction implicit finite difference scheme.[17] This finite difference scheme utilizes boundary-fitted co-ordinates and second-order-accurate finite difference approximations. The numerical grid surrounding the cylinder is subdivided into four computational domains each of resolution 41×41 or 81×81. These grids are denoted as $41 \times 41 \times 4$ and $81 \times 81 \times 4$ and should not be confused with a three-dimensional grid. Based on the finite difference simulations with the $41 \times 41 \times 4$ and $81 \times 81 \times 4$ computational grids, a conservative estimate of the accuracy of the $41 \times 41 \times 4$ finite difference simulations is 0·1 per cent.

In order to quantify the accuracy, the root mean square norm of the error in velocity and the magnitude of the maximum error in velocity are calculated. These velocity errors and their associated rates of convergence are calculated using an accurate solution, which is generated via a finely gridded lattice Boltzmann simulation using the hydrodynamic boundary condition for the octagonal cylinder and a finely gridded finite difference simulation for the circular cylinder. These velocity errors are defined as

$$\text{error norm} = \sqrt{\left(\frac{\sum[(\Delta u_x)^2 + (\Delta u_y)^2]}{\sum[(u_x^*)^2 + (u_y^*)^2]}\right)}, \tag{14}$$

$$\text{error max.} = \text{maximum } \{\sqrt{[(\Delta u_x)^2 + (\Delta u_y)^2]}\}, \tag{15}$$

where $\Delta u_x = u_x - u_x^*$, $\Delta u_y = u_y - u_y^*$ and u_x^* and u_y^* are the components of the local velocity vector normalized by the average streamwise velocity for the accurate solution. When the convergence with grid size is being examined, the sums in (14) are performed over the data points which are common to all grids. This is done in order to isolate the convergence of the solution at these fixed points in space. When examining the effects of Reynolds number or relaxation time, the sums are performed over all points in the simulation. The error in drag coefficient is defined as

$$\text{error in } C_\mathrm{d} = \left|\frac{\Delta C_\mathrm{d}}{C_\mathrm{d}^*}\right|, \tag{16}$$

where $\Delta C_\mathrm{d} = C_\mathrm{d} - C_\mathrm{d}^*$ and C_d^* is the drag coefficient obtained with the accurate simulation.

3.1. Octagonal cylinders

The two boundary conditions, i.e. the bounce-back boundary condition and the consistent hydrodynamic boundary condition, are applied at the boundaries of a periodic array of octagonal cylinders for a constant Reynolds number of 10 based on the average streamwise velocity and the

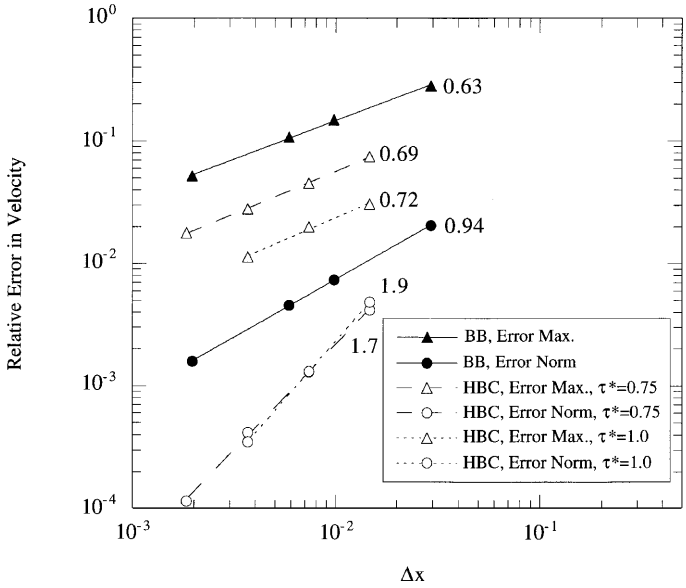

Figure 2. Errors associated with flow around a periodic array of octagonal cylinders for varying grid resolution Δx, $Re = 10$ and $\tau^* = 0{\cdot}75$. Errors are calculated for the flow around the octagonal cylinders utilizing both the bounce-back boundary condition (BB) and the consistent hydrodynamic boundary condition (HBC).[13–15] Numbers shown denote the slopes, showing the rate of convergence

width of the octagon. The associated accuracy and rates of convergence are shown in Figure 2. Here the grid spacing Δx is normalized by the domain size or, equivalently, the distance between the centre of the cylinders. The comparison with the accurate solution includes errors due to the discontinuities in slope of the octagon, contributing to the slightly sublinear convergence of the bounce-back method. The rates of convergence are 0·63 and 0·94 for the velocity error norm and maximum velocity error respectively. Formally, the bounce-back boundary condition is expected to be first-order in the vicinity of the boundary; however, it is shown here to influence the entire field, degrading the accuracy of the second-order lattice Boltzmann scheme in the entire field.

The distribution of local relative error in velocity is shown in Figure 3, where

$$\text{local error} = \sqrt{[(\Delta u_x)^2 + (\Delta u_y)^2]}. \tag{17}$$

Here the 170×170 solution using the bounce-back boundary condition is evaluated from the 1020×1020 simulation using the consistent hydrodynamic boundary condition. The maximum errors in local velocity occur at the discontinuities on the boundary of the octagonal cylinder. Although the error reaches 10 per cent, it is highly localized at the corners of the octagon, so that typical values of the local error in the flow field are less than 1 per cent.

The same measures of error used to assess flow simulations with the bounce-back boundary condition are also used to quantify errors associated with the hydrodynamic boundary condition of Noble *et al.*[13–15] Figure 2 shows the errors associated with the hydrodynamic boundary condition as a function of grid size. Here the solutions are compared with a 1088×1088 simulation using the hydrodynamic boundary condition. For two values of relaxation time, $\tau^* = 0{\cdot}75$ and 1·0, the rates of

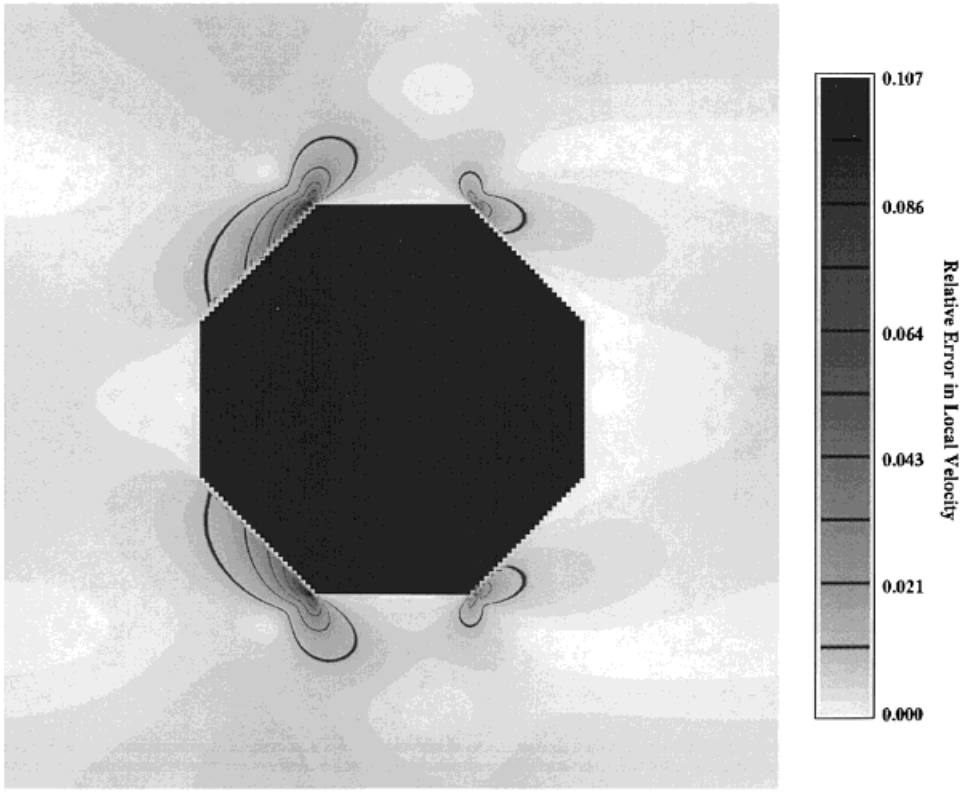

Figure 3. Distribution of local error in dimensionless velocity for $Re = 10$, $\tau^* = 0{\cdot}75$ and 170×170 computational grid. The bounce-back method is applied at the boundary of the octagonal cylinder. These velocities are compared with a finely gridded 1020×1020 lattice Boltzmann computation with the hydrodynamic boundary condition. The dark contours denote 1 per cent increments of relative velocity error

convergence are 1·7 and 1·9, respectively, for the velocity error norm and 0·69 and 0·72, respectively, for the maximum velocity error. It is noted that the convergence rate of the hydrodynamic boundary condition simulations is approximately twice that of the bounce-back simulations for the velocity error norm which gives a measure of the overall accuracy. Also, the overall velocity field converges nearly quadratically despite the fact that the maximum error is converging slowly.

The convergence of the drag force is also quantified. Figure 4 shows the relationship between grid size and relative error in the coefficient of drag. Like the errors in relative velocity, the convergence of the bounce-back simulations is sublinear, while the convergence rate of the hydrodynamic boundary condition simulations is twice that of the bounce-back simulations.

The higher rates of convergence for the hydrodynamic boundary condition occur at the relaxation time $\tau^* = 1{\cdot}0$. Field errors, including the velocity error norm and the error in drag coefficient, are decoupled from the specifics of the HBC at $\tau^* = 1{\cdot}0$, because the updated particle distribution at time $t + \Delta t$ is only determined from the equilibrium configuration and not from the specifics of the previous distribution. This is evident from (4) with $\tau^* = 1{\cdot}0$:

$$f_i(\mathbf{x} + \mathbf{e}_i \Delta t, t + \Delta t) = f_i^{\mathrm{eq}}(\mathbf{x}, t) + F_i'. \tag{18}$$

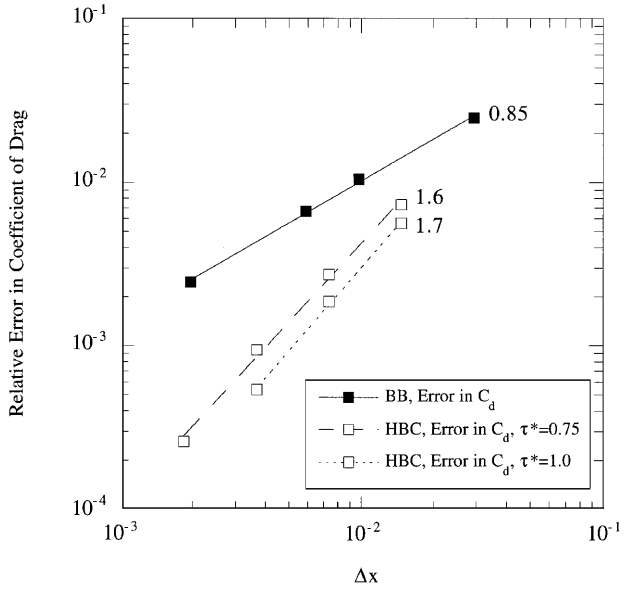

Figure 4. Relative errors in drag coefficient and convergence rates of error for lattice Boltzmann scheme for $Re = 10$ and $\tau^* = 0{\cdot}75$. The bounce-back boundary condition (BB) and the hydrodynamic boundary condition (HBC) are applied at the boundary of the octagonal cylinder. Numbers shown denote the slopes, showing the rate of convergence

For relaxation times different from unity, compressibility effects become important in the specification of boundary conditions as the velocity divergence becomes significant. It can be shown that for steady state LBM simulations[14] the internal energy is given by

$$\varepsilon = c_s - \tau c_s^2(\nabla \cdot \mathbf{u})\Delta x + O(\Delta x^2). \tag{19}$$

Because the consistent hydrodynamic boundary condition implemented on the two-dimensional square grid assumes constant internal energy,[14] the second term is neglected and additional error is introduced. As the Mach number increases, the magnitude of the divergence of velocity grows. Consequently, errors at the boundary are introduced and the apparent convergence rate decreases. This explains the lower rate of convergence for $\tau^* = 0{\cdot}75$.

The simulation accuracy as a function of Reynolds number through a periodic array of octagons is illustrated in Figure 5. The results for a 170×170 grid with the bounce-back condition applied at the boundary are compared with those for a 680×680 grid with the hydrodynamic boundary condition. The same measures of error in velocity and drag previously utilized in the evaluation of the convergence are plotted against the Reynolds number in the range from 0·1 to 100. In contrast with the flow about a single cylinder, the flow about a periodic array of cylinders is steady over this entire range of Reynolds numbers. These data display no consistent trend with Reynolds number from the Stokes regime to a Reynolds number of 100. Throughout the whole range of Reynolds numbers the errors are of the same order of magnitude but vary by a factor of up to five.

The accuracy of LBM simulations is also explicitly dependent on the relaxation time. As the relaxation time increases, the system is allowed to deviate more significantly from equilibrium and a viscosity-dependent systematic error is introduced in the flow field. Since the viscosity is a linear function of relaxation time as in (12). Figure 6 represents the relationship between error and both relaxation time and viscosity. The error associated with the bounce-back boundary condition on a 170×170 grid is compared with a 1020×1020 solution using the hydrodynamic boundary condition.

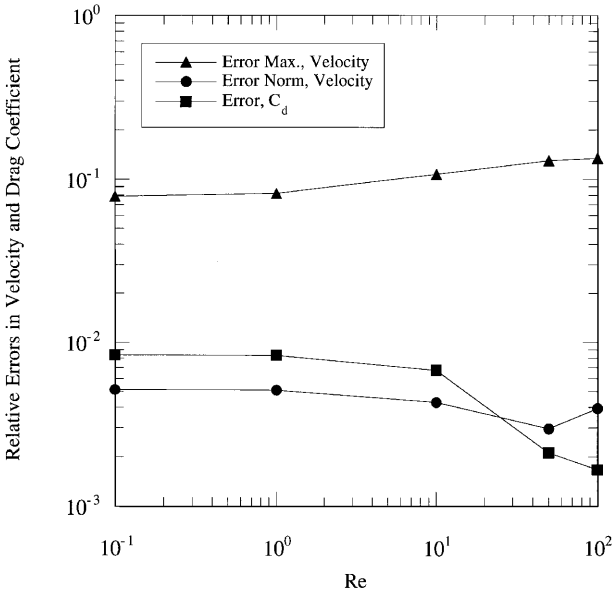

Figure 5. Relative error as a function of Reynolds number associated with two-dimensional flow around a periodic array of octagonal cylinders with bounce-back condition applied on boundary. This 170×170 grid bounce-back solution is compared with the accurate solution utilizing the consistent hydrodynamic boundary condition.[13–15] The relaxation time associated with both grids is 0·75

As shown in Figure 6, the maximum velocity error increases from 10 per cent to 30 per cent as the relaxation time increases from 0·625 to 3·5. However, this maximum velocity occurs at the discontinuities on the corners of the octagon and does not represent the bulk behaviour of the flow. Of more importance is the increase in velocity error norm and drag coefficient error with relaxation time. The magnitudes of these global errors increase nearly exponentially for relaxation times greater than unity, reaching a 2 per cent velocity error norm for a relaxation time of 3·5.

3.2. Circular cylinders

The lattice Boltzmann scheme is also applied to flow about a periodic array of circular cylinders. Because the square grid cannot perfectly simulate a curved surface, greater errors in velocity and drag are observed than in flow around the octagonal cylinder. The bounce-back method produces a stair-step boundary which is different from the continuous smooth surface of the finite difference scheme. The nature of the stair-step computational surface is shown in Figure 1. The standard accurate solution for comparison in this portion of the study is obtained with a finite difference simulation,[17] which is interpolated onto the square lattice Boltzmann grid using Shepard's method,[18,19] a smooth second-order interpolation scheme. The finite difference solution was chosen as the standard solution because the consistent hydrodynamic boundary condition, the standard in the octagonal cylinder simulations, is not readily adapted to curvilinear surfaces.

Lattice Boltzmann solutions using the bounce-back boundary condition for a range of grid spacing, Reynolds number and relaxation time are compared with the standard finite difference solution at each node and the differences in velocity are evaluated. The maximum error in velocity is identified for each simulation. Global error is represented by the norm of the velocity error and the error in the coefficient of drag. These errors are shown in Figure 7 as a function of the grid spacing. The

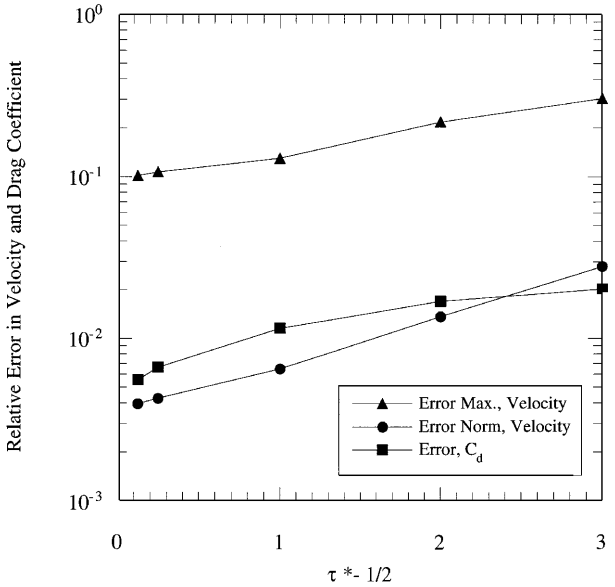

Figure 6. Comparison of relative errors in flow about octagonal cylinders as a function of relaxation time with $Re = 10$ and 170×170 grid. The errors associated with the use of the bounce-back boundary condition are calculated through a comparison with the accurate solution with the consistent hydrodynamic boundary condition[13–15]

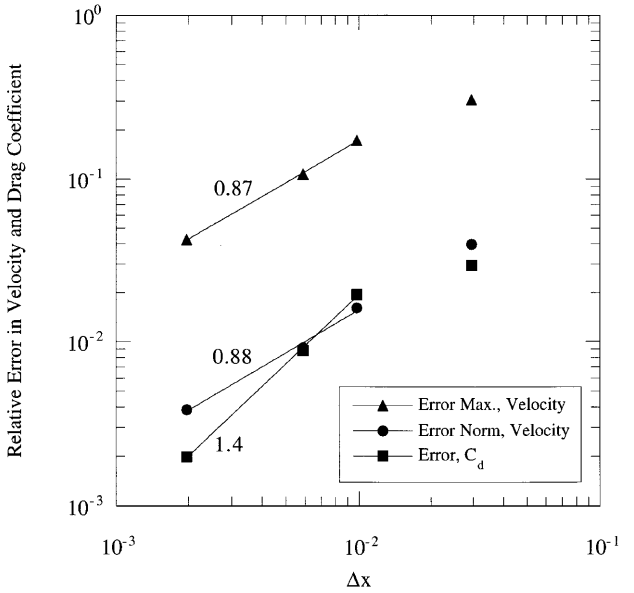

Figure 7. Relative errors in velocity and convergence rates of error as a function of grid resolution for flow about circular cylinders. The bounce-back boundary condition is applied at the cylinder boundary, with $Re = 10$ and $\tau^* = 0{\cdot}75$. The lattice Boltzmann solution is compared with an accurate finite difference solution interpolated onto a lattice Boltzmann grid. Numbers shown denote the slopes, showing the rate of convergence

magnitude of the maximum relative error is near 20 per cent for the coarsest grid, although it drops as the grid is refined, down to 4 per cent for the finest grid. The global errors in velocity and drag are significantly lower than the maximum relative velocity error, ranging from 0·3 per cent to 3 per cent for the grid sizes employed in this study.

The rates of convergence for these errors are also depicted in Figure 7. The convergence calculations do not include the values of error corresponding to the coarsest grid, since the error had not yet reached the asymptotic limit. Although the bounce-back boundary condition is formally first-order, the computed rates of convergence of velocity error are clearly below 1·0. This shows that the convergence of the simulation is reduced because the numerical grid does not conform to the curved surface of the cylinder. The slope discontinuities on the lattice Boltzmann boundary contribute to the relative error in a way which is sublinear with grid refinement.

The relative errors in velocity at each grid location in the computational domain are illustrated in Figure 8 for the 170×170 LBM simulation using the bounce-back boundary condition. The highest errors occur at the boundary of the cylinder, with the point of maximum error near the location of maximum viscous shear on the cylinder. This location also corresponds to an area where the square lattice Boltzmann grid has the highest degree of mismatch with the boundary of the cylinder. A node on this square grid has eight neighbours along horizontal, vertical and diagonal directions, so that each node is linked to neighbouring nodes at 45° increments as shown in Figure 1. As a result, the grid is particularly well suited for modelling surfaces whose tangents lie along these 45° directions.

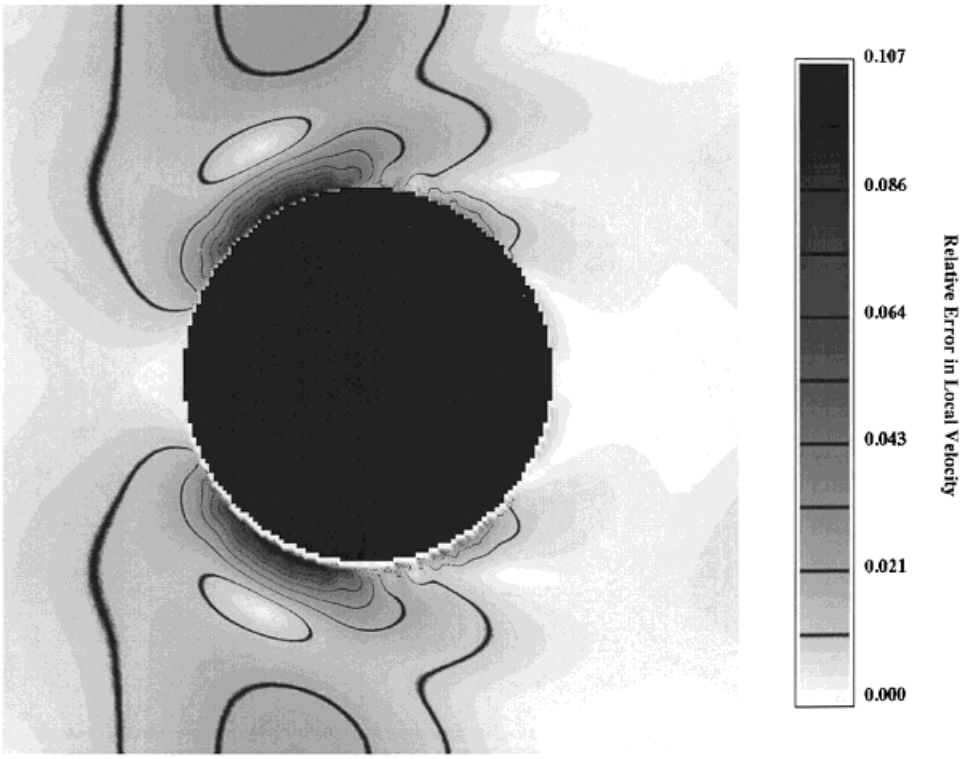

Figure 8. Distribution of local error in dimensionless velocity for $Re = 10$, $\tau^* = 0{\cdot}75$ and 170×170 computational grid. The bounce-back method is applied at the boundary of the circular cylinder. These velocities are compared with an $81 \times 81 \times 4$ finite difference computation interpolated onto the LBM grid. The dark contours denote 1 per cent increments of relative velocity error

For example, all the faces of the octagonal cylinder lie along these optimal tangent lines. The surface of the circular cylinder features tangents with varying slopes. The eight locations on the circular cylinder at 45° increments, measured radially from the centre of the obstacle and beginning with the stagnation point, are also well modelled with the LBM grid. For the same reason, boundary locations halfway between these optimal locations are not well suited for modelling with a square grid. The maximum error in relative velocity occurs at such as point, where the tangent is halfway between 0° and 45°; the error at this particular point is exacerbated by the high gradients in velocity and resulting drag associated with the behaviour of flow around a cylinder.

The total errors in total drag are represented by the coefficient of drag, discussed in the preceding paragraphs. An LBM simulation with the bounce-back boundary condition accurately predicts the coefficient of drag within 1 per cent for a 170×170 grid or finer, τ^* from 0·625 to 4·5 and Reynolds numbers between 0·1 and 50. The shear component of the total drag is also calculated from a 170×170 LBM simulation for $Re = 10$ and $\tau^* = 0{\cdot}75$. This non-dimensional shear force per unit area acting in the streamwise direction is found from[20]

$$-\frac{\omega n_y}{\frac{1}{2}Re}, \tag{20}$$

where the vorticity ω is

$$\omega = \frac{\partial u_y}{\partial x} - \frac{\partial u_x}{\partial y}. \tag{21}$$

Here the y-component of the outward-facing normal is n_y and the shear force is made non-dimensional using the size of the obstacle and the average streamwise velocity.

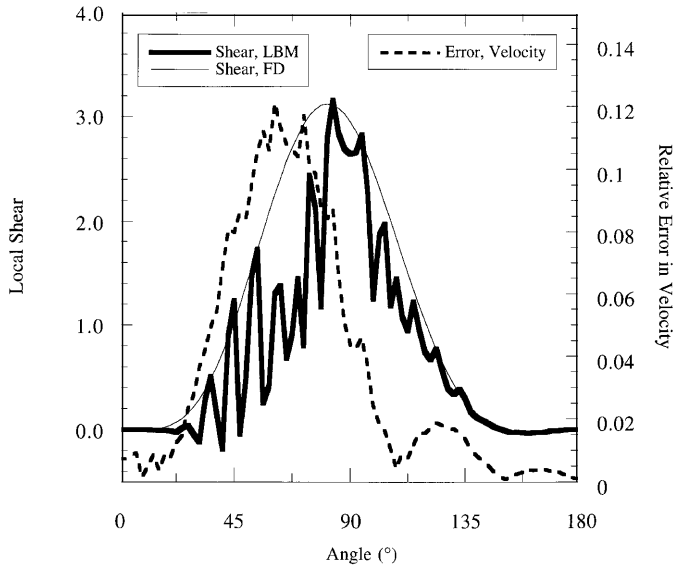

Figure 9. Local shear on surface of circular cylinder as a function of azimuthal angle, with forward stagnation point at 0°. Shear is calculated for $Re = 10$ with a 170×170 LBM simulation with $\tau^* = 0{\cdot}75$ and an $81 \times 81 \times 4$ finite difference (FD) simulation. The relative error in velocity at one node from the boundary is also shown as a function of angle

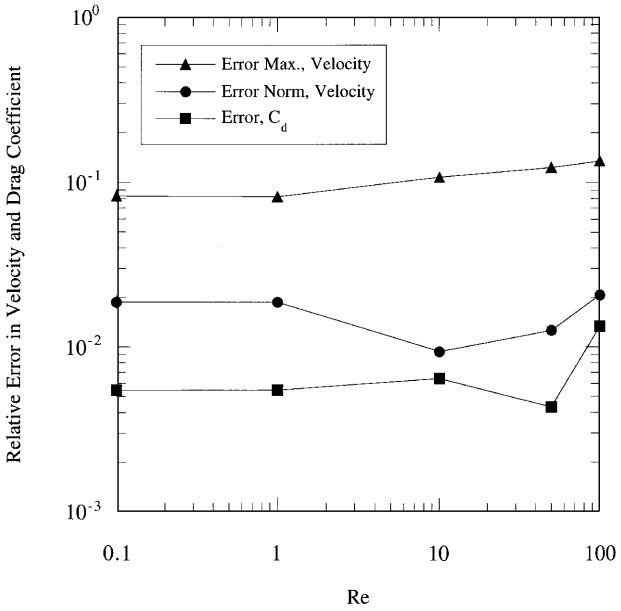

Figure 10. Comparison of relative velocity error as a function of Reynolds number for $\tau^* = 0{\cdot}75$ and 170×170 grid. The bounce-back boundary condition is imposed on the surface of the circular cylinder. The lattice Boltzmann solution is compared with the accurate interpolated finite difference solution

The shear force is calculated at each node along the obstacle boundary as a function of azimuthal angle and is shown in Figure 9. In order to compute shear for the LBM simulations, the vorticity is calculated at each node from the velocity field using second-order-accurate finite differences according to (21). The vorticity is then interpolated onto the finite difference grid by Shepard's method.[18,19] The deviation between the finite difference and interpolated LBM solutions shows that the LBM simulation fails to represent the local shear at each boundary node, although the shear is considerably more accurate at boundary locations where the slope of the cylinder is approximated by the LBM grid. The error in local relative velocity near the obstacle is also shown in Figure 9. This is the error in velocity one node outside the obstacle as a function of angle. It is observed that the largest deviation in shear force occurs when this local velocity error is greatest, not when the shear force is maximum. Consequently, the LBM with the bounce-back boundary condition does not accurately predict local shear owing to the stair-step nature of the boundary and the errors in local velocity near the boundary. However, as shown in Figure 7, this method accurately predicts total drag, recovering the global behaviour of the bulk of the flow.

The errors in relative velocity and drag force are a much stronger function of grid size than Reynolds number. The effects of Reynolds number on maximum relative error in velocity, velocity error norm and error in coefficient of drag are shown in Figure 10 for $Re = 0{\cdot}1$ up to 100 and a 170×170 grid. The maximum error varies between 8 per cent and 11 per cent, increasing with Reynolds number. Errors in velocity norm range from 0·8 per cent up to 2 per cent, with a minimum near $Re = 10$. The errors in the drag coefficient are smaller than the velocity errors, ranging between 0·4 per cent and 2 per cent.

Errors in velocity also vary with relaxation time as the solution deviates further from equilibrium. Figure 11 depicts the effects of relaxation time on maximum velocity, velocity norm and drag coefficient. For relaxation times less than 1·5 the error remains relatively constant, except for the

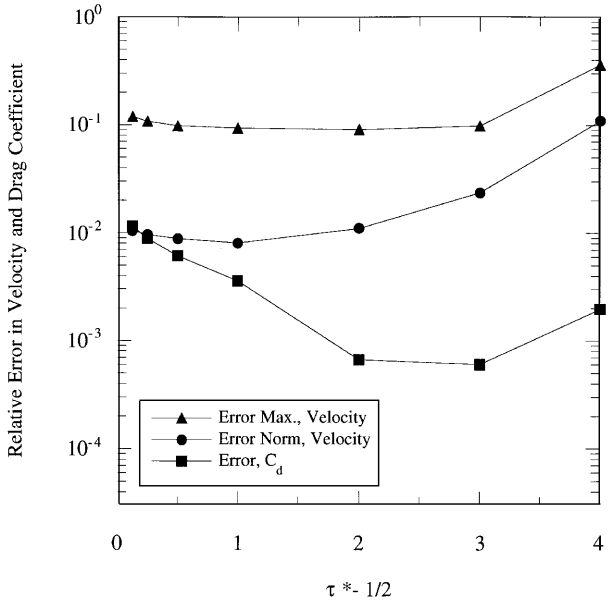

Figure 11. Relative velocity errors associated with bounce-back boundary condition for flow around an array of circular cylinders as a function of relaxation time. This 170×170 lattice Boltzmann grid is compared with the accurate finite difference calculation at $Re = 10$

error in the drag coefficient, which decreases. However, for greater values of relaxation time the error begins to increase exponentially. For sufficiently small values of τ^* the errors are not a strong function of relaxation time. Beyond this region of short relaxation times the error is strongly dependent on τ^*.

4. CONCLUSIONS

The bounce-back boundary condition is shown to be a reasonably accurate method for modelling the boundary of octagonal and circular cylinders in lattice Boltzmann simulations of hydrodynamics for a range of discretization parameters. With a 170×170 grid the lattice Boltzmann simulations prescribed here are accurate for relaxation times less than 1·5 and Reynolds numbers between 0·1 and 100. The root mean square norm of the velocity error and the error in drag coefficient are less than 1 per cent for the octagonal cylinder and 2 per cent for the circular cylinder.

The octagonal cylinder conforms well to this square grid and maximum relative velocity errors occur in small, localized regions at the discontinuities, or corners, of the octagon. However, the circular cylinders does not conform to the square LBM grid. The areas on the cylinder which least conform to the square grid are the locations of maximum relative velocity error, which propagates outwards into the flow field. Although the maximum errors in relative velocity are of the same magnitude for octagonal and circular cylinders, the error norm and drag coefficient error for the circular cylinder are twice as large as those for the octagonal cylinder, since the errors associated with the octagonal cylinders only exist near the boundary, while the errors of the circular cylinder affect the entire flow. The convergence rates of these errors are near first-order for both the octagonal and circular cylinders.

Although the error inherent in the bounce-back method is higher than that associated with the consistent hydrodynamic boundary condition and the rate of convergence is slower, the bounce-back boundary condition provides a computationally efficient method for a curved surface.

ACKNOWLEDGEMENTS

This research is supported by a National Science Foundation Graduate Fellowship, NCSA grant CBT-930030N, NSF CTS 95-21509 and the Richard W. Kritzer Foundation. All lattice Boltzmann simulations reported here were performed on the CM-5 of the National Center for Supercomputing Applications. The authors would like to thank Dr. M. Wang for the use of the finite difference code.

REFERENCES

1. G. McNamara and G. Zanetti, 'Use of the Boltzmann equation to simulate lattice-gas automata', *Phys. Rev. Lett.*, **61**, 2332–2335 (1988).
2. F. Higuera and J. Jimenez, 'Lattice gas dynamics with enhanced collisions', *Europhys. Lett.*, **9**, 663–668 (1989).
3. H. Chen, S. Chen and W. H. Matthaeus, 'Recovery of the Navier–Stokes equations using a lattice Boltzmann method', *Phys. Rev. A*, **45**, R5339–R5342 (1991).
4. S. Y. Chen, H. D. Chen, D. Martinez and W. Matthaeus, 'Lattice Boltzmann model for simulation of magnetohydrodynamics', *Phys. Rev. Lett.*, **67**, 3776–3779 (1991).
5. Y. H. Qian, D. d'Humières and P. Lallemand, 'Lattice BGK models for the Navier–Stokes equation', *Europhys. Lett.*, **17**, 479–484 (1992).
6. D. d'Humières and P. Lallemand, 'Numerical simulations of hydrodynamics with lattice gas automata in two dimensions', *Complex Syst.*, **1**, 599–632 (1987).
7. R. Cornubert, D. d'Humières and D. Levermore, 'A Knudsen layer theory for lattice gases', *Physica D*, **47**, 241–259 (1991).
8. I. Ginzbourg and P. M. Adler, 'Boundary flow condition analysis for the three-dimensional lattice Boltzmann model', *J. Phys. II Fr.*, **4**, 191–214 (1994).
9. D. P. Ziegler, 'Boundary conditions for lattice Boltzmann simulations', *J. Stat. Phys.*, **71**, 1171–1177 (1993).
10. P. A. Skordos, 'Initial and boundary conditions for the lattice Boltzmann method', *Phys. Rev. E*, **48**, 4823–4842 (1993).
11. T. Inamuro, M. Yoshino and G. Ogino, 'Non-slip boundary condition for lattice Boltzmann simulations', *Phys. Fluids*, **7**, 2928–2930 (1995).
12. S. Chen and D. Martinez, 'On boundary conditions in lattice Boltzmann methods', *Phys. Fluids*, submitted.
13. D. R. Noble, S. Chen, J. G. Georgiadis and R. O. Buckius, 'A consistent hydrodynamic boundary condition for the lattice Boltzmann method', *Phys. Fluids*, **7**, 203–209 (1995).
14. D. R. Noble, J. G. Georgiadis and R. O. Buckius, 'Direct assessment of lattice Boltzmann hydrodynamics and boundary conditions for recirculating flows', *J. Stat. Phys.*, **81**, 17–33 (1995).
15. D. R. Noble, J. G. Georgiadis and R. O. Buckius, 'Comparison of accuracy and performance for lattice Boltzmann and finite difference simulations of steady viscous flow', *Int. J. Numer. Meth. Fluids*, **23**, 1–18 (1996).
16. P. Bhatnagar, E. P. Gross and M. K. Krook, 'A model for collision processes in gases. I. Small amplitude processes in charged and neutral one-component systems', *Phys. Rev.*, **94**, 511–525 (1954).
17. M. Wang and J. G. Georgiadis, 'Conjugate forced convection in crossflow over a cylinder array with volumetric heating', *Int. J. Heat Mass Transfer*, **39**, 1351–1361 (1996).
18. D. Shepard, 'A two-dimensional interpolation function for irregularly spaced data', *Proc. 23rd Nat. Conf. of ACM*, 1968, pp. 517–523.
19. R. J. Renka, 'Multivariate interpolation of large sets of scattered data', *ACM Trans. Math. Softw.*, **14**, 139–148 (1988).
20. G. K. Batchelor, *An Introduction to Fluid Dynamics*, Cambridge University Press, Cambridge, 1967.

